Parametric Study of Design Options affecting Solid Rocket Motor Start-up and Onset of Pressure Oscillations

M. Di Giacinto[a,*], E. Cavallini[a,**], B. Favini[a], J. Steelant[b]

[a]*Sapienza University of Rome - Dept. of Mechanical and Aerospace Engineering, Via Eudossiana 18, 00184 - Rome, Italy*
[b]*ESA-ESTEC - TEC-MPA, Keplerlaan, 1 - 2201 AZ Noordwijk, The Netherlands*

Abstract

The start-up represents a very critical phase during the whole operational life of solid rocket motors. This paper provides a detailed study of the effects on the ignition transient of the main design parameters of solid propellant motors. The analysis is made with the use of a Q1D unsteady model of solid rocket ignition transient, extensively validated in the frame of the VEGA program, for ignition transient predictions and reconstructions, during the last ten years. Two baseline solid rocket motor configurations are selected for the parametric analysis: a big-booster with a three-segments propellant grain shape, similar to Ariane 5, and a small-booster/solid stage with an aft-finocyl grain shape, similar to VEGA solid rocket motors. The discussion of the results is particularly addressed on the possible onset of pressure oscillations during the start-up of the two solid rocket motor configurations, pointing out the design parameters which affect them in terms of occurrence and amplitude.

Keywords: solid rocket motors; ignition transient; design options; parametric analysis.

1. Introduction

The Ignition Transient (IT) of Solid Rocket Motors (SRMs) is characterized by strong unsteady phenomena occurring in a very short period of time. It starts at the first electric signal given to the igniter charge and ends after the ignition of the entire grain surface, when the quasi steady state conditions in the bore are reached (usually after from 0.2 to 1 s, depending on motor size and configuration). In spite of the short period of time taken by this operative phase, its impact on the launch system design and operation can be relevant. In fact, the IT has significant implications not only from the point of view of the SRM start-up and the thrust delivered by the SRM during this crucial operative phase, but also for the launch vehicle operational requirements and structural verifications. Therefore, the development of new SRMs requires to improve the understanding of the IT physical mechanisms and to clarify their origins and dependencies. Moreover, the availability of reliable and efficient IT simulation models, able to properly predict and analyze the SRM behavior, may make possible the accomplishment of the system requirements already from the preliminary design phase of the SRM. Indeed, many times unacceptable IT behaviors were detected at an advanced development stage (i.e. at the first static firing tests), when remedies and/or design modifications could be very expensive and with a big impact on the project time schedule.

Aim of this study is to present a wide parametric analysis of the effects of the main SRM design options on the SRM start-up phase, with a particular attention on the onset of pressure oscillations. This work exploits all the experience and know-how achieved at the Sapienza University of Rome, by the research group of solid rocket propulsion, in the simulations of the start-up phase of solid rockets, especially in the frame of the VEGA programme, during the development of the solid stages.

This paper is structured as follows. Firstly, in section 2, a brief description of the model used for the parametric analysis, named SPIT (Solid Propellant rocket motor Ignition Transient) is provided. Then, section 3 describes the two baseline SRM configurations considered in the parametric analysis: a three-segment booster and a smaller finocyl SRM. The ignition transient of both the SRM baseline configurations is analyzed in details in section 4. Then, the description design options varied in the parametric analysis and the effects of each design option on the motor ignition transient are depicted in section 5.

2. Q1D SRM Ignition Transient Model

This section describes the Q1D unsteady model of SRM ignition transient (named SPIT - Solid Propellant rocket motor Ignition Transient), used for the accomplishment of the parametric analysis presented in this work. This model was successfully validated against all the European SRMs (Ariane 4, Ariane 5, Zefiro 9, Zefiro 16, Zefiro 23 and P80FW) and largely adopted in the frame of the VEGA programme, for the predictions and reconstructions analyses of the solid stages ignition transient [1–15].

The gasdynamic model is an unsteady quasi-1D Euler flow model, with mass momentum and energy source terms, in order

*Passed away on May, 2nd 2013.
**Corresponding author.
Email addresses: maurizio.digiacinto@uniroma1.it (M. Di Giacinto), enrico.cavallini@uniroma1.it (E. Cavallini), bernardo.favini@uniroma1.it (B. Favini), johan.steelant@esa.int (J. Steelant)

to account for the igniter, the propellant grain mass addition due to combustion and coupling terms between the core flowfield and motor cavities, such as slots, submergence and floaters. The governing equations for the flowfield are written for a single phase, non-reacting mixture of perfect gases, since very fast chemical reactions are assumed to occur in a ideal thin layer at the propellant surface.

The possible presence of slots, floaters and the submergence region (so called "cavity regions") is not considered in the cross sectional area of the Q1D representation of the SRM, and their effects are accounted for by a dedicated sub-model (cavity model), which considers mass and energy exchange terms with the main flow. The cavity model is based on a set of ordinary differential equations deduced from a volume averaging of the mass and the energy conservation equations, accounting for source terms which describe the presence of burning combustion surface in the cavity and the mass and energy exchange with the main flow (Q1D model of the SRM flowfield).

The initial conditions are defined by the initial geometry of the propellant surface, the initial state of the pressurizing gas inside the combustion chamber and the ambient conditions inside the diverging portion of the nozzle.

The wall boundary condition is assumed at both the head-end of the motor and nozzle throat, until the seal breakage (in case of the classical presence of a seal protecting the SRM combustion chamber from the external environment). Then, at the occurrence of the nozzle seal rupture, the outside pressure value is imposed at the exit section of the diverging nozzle, until the supersonic flow conditions at the nozzle end are acquired.

The evaluation of the time history of the propellant surface temperature is obtained using an ordinary differential equation derived from the coupling the unsteady 1D Fourier equation and the gas-solid heat convection equation. The ignition criterion is based on the assumption that the ignition of the combustion takes place when the surface temperature reaches an assigned value, which depends on the local pressure at the propellant grain surface.

For the igniter model, the influence of its design parameters and operative conditions on the motor start-up are considered in terms of: the overall igniter design options (external shape, dimension and location inside the motor chamber); the igniter nozzle design options (number, shape, dimension, location and orientation); the igniter operational design options (thermodynamic data of the igniter combustion products and time evolution of the pressure inside the igniter, or any equivalent information in order to set boundary conditions for igniter nozzles).

Semi-empirical models are applied for the estimation of the location and the dimensions of the impingement region on the propellant surface, as well as for the evaluation of the heat transfer coefficient, in the impingement region and in the remaining propellant grain surface. The adopted burning rate model is based on the de Saint Robert-Vieille, for the quasi steady term and on the Lenoir-Robillard model, with the further modifications proposed by Lawrence and Lamberty, for the erosive burning term.

The discretized model is based on an equally spaced finite volume approximation of the conservation equations, recast in integral form. The adopted numerical method is a second order accurate ENO method, coupled with an exact Riemann solver. A full description of the models and sub-models is not in the scope of this work and can be found in Refs. [1–5].

3. Definition of Baseline Configurations of SRMs for Parametric Analysis

Two reference configurations are chosen for the parametric analysis. These two baseline motors are selected because belonging to different SRM designs for launcher applications (a booster and a stage/small booster), similar in terms of design, respectively to a Ariane 5 solid booster and a VEGA solid stage. The first baseline configuration (SRM `A`) is a three-segments SRM, whereas the second one (SRM `B`) is an aft-finocyl SRM. Both the SRMs have a submersed nozzle configuration.

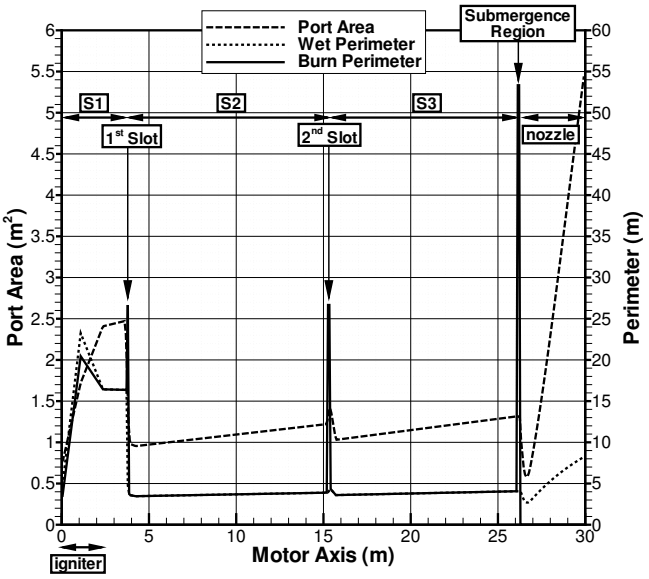

Figure 1: Geometric Configuration of Segmented SRM `A`

Figure 1 and figure 2 show the port area (left axis), wet and burning perimeter (right axis) against the SRM axis, for the SRM `A` and SRM `B` respectively.

Similarly to Ariane 5 SRM geometry, the baseline SRM `A` has the first segment (`S1`) with a star shaped like geometry, whereas the second and the third segments (`S2` and `S3`) are shaped axisymmetric, with a small angle of tapering. For the `S1`, in order to mimic a star shaped region in a simplified manner, an artificial increase of the wet and burning perimeter is considered (see Fig. 1), in order to have an initial Klemmung number for the SRM of about 250 (which represent a typical value for such kind of motor).

For the baseline SRM `B`, the finocyl propellant grain geometry, composed by a tapered geometry at the SRM head-end connected with the aft-finocyl region, is modeled with an increase of the burning and wet perimeter in the aft-end of the SRM, with a smooth transition between the cylindrical tapered region and the finocyl one (see Fig. 2). The Klemmung number for the SRM `B` is about 220.

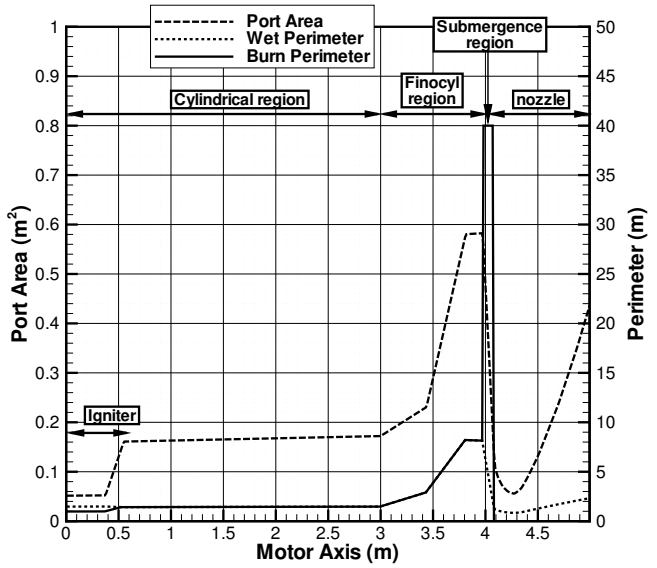

Figure 2: Geometric Configuration of Finocyl SRM B

In the Q1D representation of the SRMs geometry, the burning areas in the submergence regions (for both the baseline SRM A and B) and the slots are modeled with a local increment of the burning perimeter, as depicted in Fig. 1 and Fig. 2.

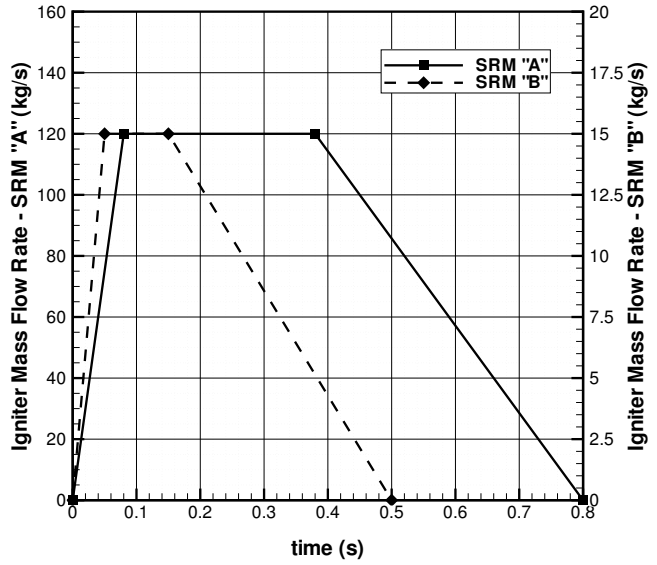

Figure 3: Igniter Mass Flow Rate Variation in Time for SRM A and B

In order to simplify the set-up of the igniter operative conditions, the igniter mass and energy addition is imposed, since the igniters are assumed to be, as typical for these kind of SRMs, pyrogen type igniters. The igniter mass flow rate law in time is assumed to be composed by, as typical for SRMs, a rapid grow up, followed by a constant interval and a slow decay, as given in Fig. 3. A different overall mass of the igniter charge and igniter operative time are assumed for the SRM A and the SRM B, typical for the SRMs under study.

The igniter combustion products adiabatic flame temperature and gas properties are evaluated by CEA code[16], from typical compositions of the igniter propellants. In Tab. 1, the main data of the igniter configurations for the SRM A and SRM B are reported.

Table 1: Igniter Input Data for SRM A and SRM B

	SRM A	SRM B
No. Canted Nozzles	5	3
Canting Angle, (deg)	45	35
No. Axial Nozzles	0	0
Nozzle Throat Radius (m)	0.035	0.015
Length (m)	0.45	0.55
Radius (m)	0.2	0.1
Total Temperature (K)	3300	3300
Specific Heat Ratio	1.14	1.14
Molecular Weight (g/mol)	29	29

Both the SRMs are designed with the presence of a seal located at the nozzle throat, which breaks during the SRM start-up at an imposed differential pressure value (4 bar for the SRM A and 6 bar for the SRM B). Both the SRMs are considered filled by nitrogen, as pressurizing gas, initially at rest, at ambient conditions and at a pressure of 1.3 bar.

The input data for the propellants of the two SRMs are given in Tab. 2, as typical for the two baseline SRMs.

Table 2: Propellant Input Data for SRM A and B

	SRM A	SRM B
Density (kg/m^3)	1800	1800
Flame Temperature, (K)	3100	3100
Burning Rate @ 60 bar (mm/s)	≈ 6	≈ 10
Burning Rate Exponent	0.4	0.4

In order to assess qualitatively and quantitatively the onset and the characteristics of the pressure oscillations during the SRM start-up, the baseline configurations are intentionally chosen such that: the SRM A is not prone to relevant pressure oscillations during the start-up; whereas the SRM B is properly intended to be subjected to pressure oscillations during the first phase of the ignition transient.

The reference parameter that will be shown and compared for all the numerical simulations in the analysis is the SRM head-end pressure (HEP) trend over time, as representative of all the events occurring in the SRM combustion chamber.

For a deepened discussion about the root mechanism underlying the onset of pressure oscillations in finocyl SRMs and some possible remedies theoretically discovered in the recent past and successfully used in the frame of the VEGA program, the interested reader can refer to Refs. [6–11, 13, 14, 17–22].

4. Analysis of Baseline SRMs Ignition Transient

4.1. Segmented SRM

Figure 4 shows the head-end pressure variation in time of SRM A during the whole ignition transient. Figure 4 presents also a detailed view of the pressure trend, during the first time

instants of the motor start-up (also called pre-ignition transient phase - pre-IT).

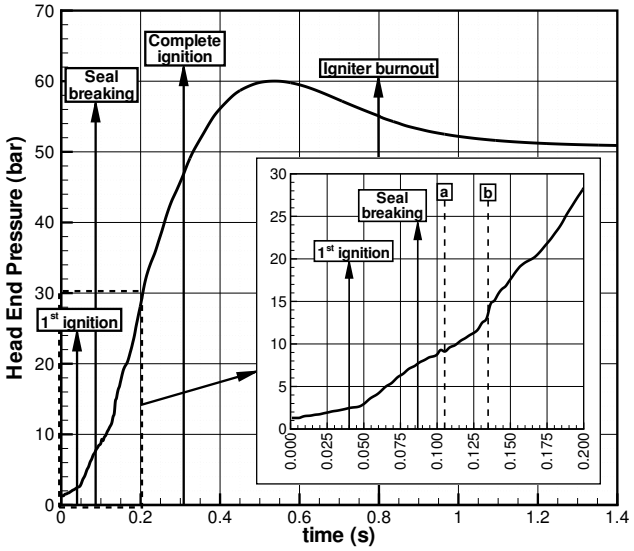

Figure 4: Head End Pressure during Start-up of SRM A

In Fig. 4, some typical events of the ignition transient are highlighted: the time instant of the first ignition of the propellant grain surface, the seal breaking up time, the time of complete ignition of the combustion surface, and the time of igniter burnout, as given by the imposed law for the igniter mass flow rate (see Fig. 3). As evident looking at both Fig. 4, the SRM ignition transient is not characterized by pressure oscillations during the first part of the ignition transient.

Besides this fact, the HEP is characterized by other four main events grouped into the following two time intervals.

The first one is at ≈ 0.1 - 0.11 s, which corresponds to the ignition of the first slot and the almost simultaneous footprint on the HEP of the reflection of a compression wave on the head end of the motor, with the curve knee evident in Figure 4 ("a" flag). This compression is the result of the following chain of events: a strong compression, triggered by the igniter, moves from the head end towards the aft end of the SRM; it raises the pressure in the SRM aft part, is reflected by the nozzle seal and causes the nozzle seal breakage (about half acoustic time before its footprint on the HEP - "a" flag in Figure 4). The reflected compression wave moves again towards the head end of the SRM, with complex interactions with the submergence region, the slots, the geometrical variation of the bore and the igniter jets contact discontinuities (forward and aft front). When this compression wave reaches the head end of the SRM, it leaves the footprint shown as flag "a" in the HEP curve (see Fig. 4).

The second time interval which merits to be analyzed and discussed occurs at ≈ 0.13 - 0.14 s ("b" flag on Figure 4), when the following concurrent events take place: the start of the ignition of the head end of the SRM and the simultaneous completion of the flame spreading in the SRM aft end. During this last phase, because of the nozzle seal rupture, a slow and low amplitude excitement of the SRM first longitudinal acoustic mode is present in the head-end pressure profile, up to ≈ 0.5 s, during the rapid chamber pressure growth. Then, a classical shape of the HEP is shown during the chamber filling phase, with a typical pressure overshoot, up to the reaching of the quasi-steady pressure. This pressure overshoot is dictated by a relevant erosive burning in the impingement region caused by the igniter jets, concurrent with the mass addition into the chamber due to the tail off phase of the igniter (that burns out at 0.8 s - Fig. 3).

4.2. Finocyl SRM

As for the SRM A, Figure 5 shows the HEP time history during the whole ignition transient, whereas a detailed view of the first part of the ignition transient is provided in the box of Fig. 5. As evident in Fig. 5, this second baseline SRM is prone to the presence of relevant pressure oscillations during the first part of the ignition transient. In particular, these pressure oscillations occur after the first ignition of the propellant grain and before the nozzle seal breaking.

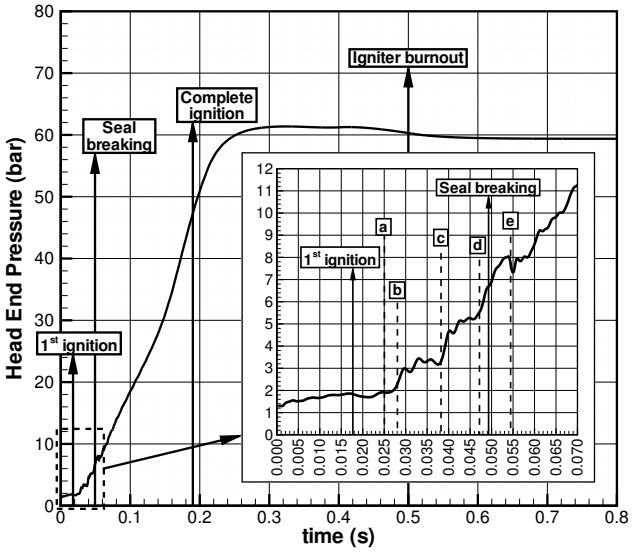

Figure 5: Head End Pressure during Start-up for SRM B

The mechanism of onset of this kind of pressure oscillations has been widely and deeply analyzed during the last years by the solid rocket work-group at Sapienza University of Rome and discussed in several papers published in the literature, see Refs.[6–11, 13, 14, 17–22]. Therefore, in this paper, the physics underlying these phenomena will be only briefly summarized.

The mechanism that drives the origin of pressure oscillations is related to a pure gasdynamic phenomenon due to the interaction between the igniter jets and the port area variation of the aft-finocyl region. This interaction triggers the onset of acoustic waves traveling into the combustion chamber and brings about the excitement of the chamber first acoustic mode [8, 9, 18]. In particular, the triggering cause for the chamber first acoustic mode excitation is rooted into the interaction of the igniter jets material surface with the aft-finocyl entrance region (at ≈ 0.026 s - "a" flag in Figure 5), which generates a system of complex rarefaction/compression waves [8, 9, 18]. The first one is

a pressure wave which propagates back to the head-end motor (reached at ≈ 0.0275 s - "b" flag in Figure 5).

Whereas the second one is a compression wave that travels towards nozzle. This latter compression wave is then reflected by the nozzle seal, reaches the head end at ≈ 0.0375 s ("c" flag in Fig. 5) and it is reflected again. Then, the resulting wave moves towards the nozzle seal, from which is one more time reflected, heading towards the SRM head end, which is reached at ≈ 0.475 s ("d" flag in Figure 5), slightly before the nozzle seal rupture.

These events are manifested on the head-end pressure time history as relevant pressure fluctuations (see Fig. 5). Even if for this kind of SRM configuration the first ignition of the propellant grain combustion surface occurs before the first onset of the pressure oscillations, no role is played in the root cause of the onset of the pressure oscillations by the propellant grain ignition and combustion.
The nozzle seal rupture occurs at ≈ 0.049 s and it is recorded in the HEP after half acoustic time (≈ 0.005 s) at ≈ 0.054 s, bringing about a knee in the HEP curve ("e" flag in Figure 5). Afterwards, with reference to Figure 5, a rapid flame spreading and, hence, the chamber pressurization occurs and the pressure oscillations are suddenly damped. The propellant ignition spreads up to the finocyl region and the head end region, at approximately 0.2 seconds. Then, the chamber filling phase occurs until the reaching of the quasi-steady conditions. For the reference case B, this phase of the IT is less affected by the erosive burning effects, with a lower pressure over-peak, in comparison with the reference case A.

5. Parametric Analysis

5.1. Test Matrix of SRM Design Options

The parametric analysis considers a wide test matrix that considers the variation of all the main design parameters of the SRM which play a role in the start-up:

- **Propellant Grain Shape and Geometry**:
  - for SRM A (AMSG1 case), the change of design of the propellant grain consists in a monolithic 2D star-shaped grain (with a constant geometry along the SRM axis), with the same bore volume and the same overall combustion surface of the baseline (the inter-segment slots and the submergence region are removed, but the SRM has the same head-to-throat length);
  - for SRM B (BMSG1 case), the change of design of the propellant shape considers a monolithic 2D star shaped grain (with a constant geometry along the SRM axis) with the same bore volume, overall combustion surface, and SRM head-to-throat length.
- **Igniter Configuration**: the modification of the igniter configuration consists in the addition of an axial nozzle to the baseline SRM A and B. The igniter mass flow rate distribution is imposed 50%(canted)-50%(axial) among the axial and the canted nozzles (named AIC1 case for SRM A and BIC1 case for SRM B).
- **Pressurizing Gas Type**:
  - helium, instead of the baseline nitrogen (named APGT1 case for SRM A and BPGT1 case for SRM B);
  - mixture of 50 % helium and 50 % nitrogen in mass (APGT2 case for SRM A and BPGT2 case for SRM B).
- **Igniter Gas Total Temperature**: variation of the total temperature of the igniter combustion products - more and less energetic igniter (2500 and 4000 K will be considered, respectively cases AIGT1, AIGT2, for SRM A and BIGT1, BIGT2, for SRM B).
- **Propellant Grain Products Total Temperature**: modification of the total temperature of the grain combustion products - more and less energetic propellant grain (2500 and 4000 K will be considered, respectively cases AGPT1, AGPT2, for SRM A and BGPT1, BGPT2, for SRM B).
- **Ballistics Propellant Properties**: variation of the burning rate of the propellant grain (faster and slower combustion rate ± 20 %, ABPP1, ABPP2, for SRM A and BBPP1, BBPP2, for SRM B).
- **Igniter Mass Flow Rate Time History**: the igniter MFR time history shown in Fig. 3 is modified in the maximum MFR value. Accordingly, also the Δt shown in Fig. 3 will be varied in order to keep constant the overall functioning time and igniter propellant mass. Two cases are considered for each baseline configuration: higher (130 % - AMFR1 and BMFR1) and lower (80 % - AMFR2 and BMFR2) maximum mass flow rate.
- **Initial Pressurization Level**: increase of the SRM initial pressurization level to 2.5 bar for both the baseline SRMs (named case AGPL1 for SRM A and BGPL2 for SRM B), instead of the reference value of 1.3 bar.
- **Seal Diaphragm Breakage Level**: variation of the diaphragm breaking up level:
  - open chamber configuration (cases ADBL1 for SRM A and BDBL1 for SRM B) - no nozzle diaphragm;
  - higher breakage level of the nozzle seal - 8 bar for both the SRMs (i.e. 7 bar of differential pressure of breakage among the inner and the outer of the SRM chamber - cases ADBL2 for SRM A and BDBL2 for SRM B).

5.2. Results of Parametric Analysis

The discussion of the results is divided in two parts. In the first one, some general effects on the ignition transient, in common for both the SRM baseline configurations are discussed. In the second part, the discussion is more focused on the effects of SRM design parameters on the onset, increase/decrease of pressure oscillations phenomena during the SRM start-up.

The variation of the propellant grain shape geometry (cases AMSG1 and BMSG1 - see Fig. 6 and Fig. 7) represents, for both the SRMs, a complete redesign of the SRM configuration, that is proposed and made with the only purpose to focus the attention on the effects on the pressure oscillations during the SRM start-up of the internal profile of the SRM combustion chamber. For these reasons, these cases will be discussed only in the second part of the results analysis of the analysis of the results.

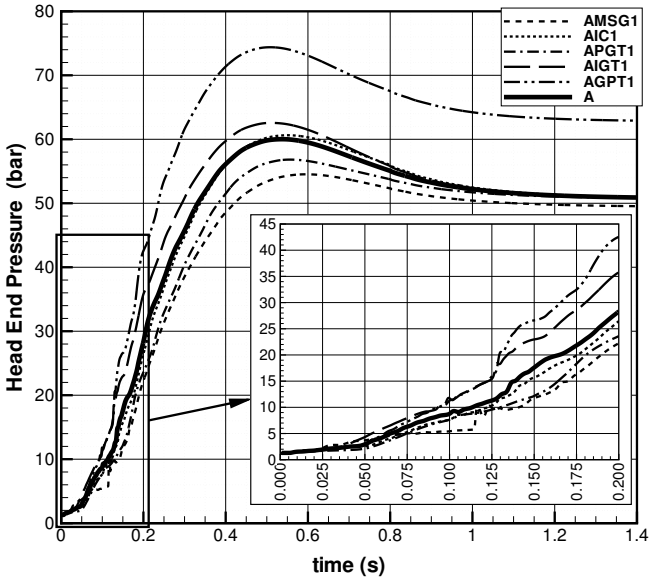

Figure 6: Head End Pressure during Start-up for SRM A - Parametric Analysis

A more energetic igniter (cases AIGT1 and BIGT2 - see Fig. 6 and Fig. 7) brings to a more rapid ignition of the SRM and, consequently, to a higher pressure growth rate during the IT. In fact, a higher value of the igniter total temperature defines an increase of the heat fluxes of the impingement region and hence, an early ignition of the impingement zone of the propellant surface. Concurrently, because of the higher total temperature, for the same mass flow rate law in time of the igniter, a slight enlargement of the impingement region occurs. Moreover, an early occurrence of the seal breaking takes place, due to the more intense train of compression waves generated by itself at the start-up. As expected, there are no effects on the quasi steady pressure reached by the SRM, at the end of the ignition transient. However, the ignition transient is characterized by a higher pressure overshooting, because of an enhancement of the erosive burning within the impingement region (higher convective heat fluxes, that enhances the burning rate of the propellant grain). The opposite effects stand in case of a reduction of the igniter energy for the cases AIGT2 and BIGT2.

A more energetic propellant (cases AGPT1 and BGPT1 - see Fig. 6 and Fig. 7 does not alter, as expected, the first part of the ignition of the propellant surface. Afterwards, because of the different chemical energy of the propellant, all the more the grain propellant surface is ignited, all the more the variation of the propellant flame temperature brings to higher pressure values inside the chamber. This in turn, affecting the flow field temperature and the radiation from the ignited regions of the propellant surface, implies an augmentation of the heat fluxes towards the unignited propellant regions and, hence, brings about a more rapid propellant ignition (with a slight increase of the flame spreading velocity along the motor axis). As a consequence, the obtained higher pressure growing rate defines also a more rapid time of ignition of the whole SRM burning surface. In the same time, as expected, a more energetic propellant enhances the quasi steady pressure reached at the end of the IT and the pressure growth rate. As for the previous case, the opposite remarks stands for the cases AGPT2 and BGPT2.

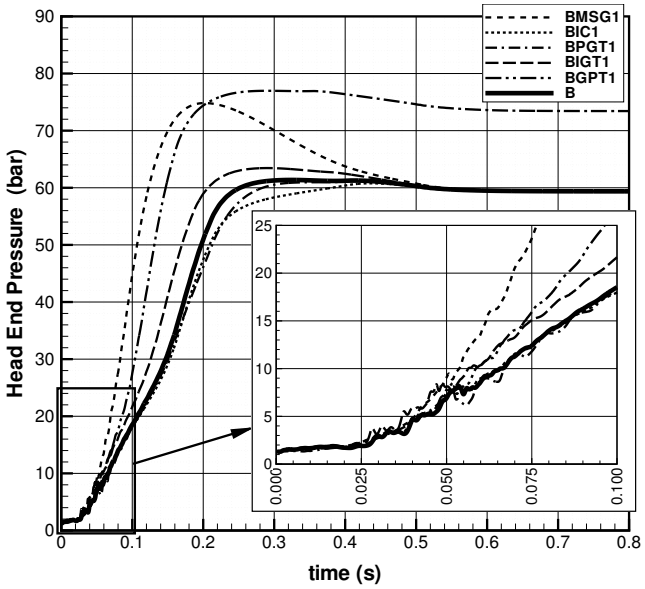

Figure 7: Head End Pressure during Start-up for SRM B - Parametric Analysis

A propellant with a faster combustion velocity (cases ABPP1 and BBPP1 - see Fig. 8, and Fig. 9) has not any relevant effect on the ignition sequence of the propellant grain surface, since it does not modify in a relevant manner the flame spreading along the combustion surface. The exception is the head end region of the SRM, where the ignition occurs at a later time during the IT and, therefore, the dependence of the ignition temperature from the pressure plays a role. In fact, a faster propellant grain enhances the quasi steady pressure reached at the end of the IT and consequently the pressure growth rate during the SRM start-up. In the same time, because of the higher pressure in the chamber, it reduces the pressure overpeak during the last part of the ignition transient, since a reduction of the erosive burning effects in the impingement region occurs. The opposite remarks can be turned out for the ABPP2 and the BBPP2 cases.

A different igniter mass flow rate (MFR) distribution in time (higher maximum MFR value for the same overall igniter mass - cases AMFR1 and BMFR1, see Fig. 8 and Fig. 9) decreases the ignition time of the entire propellant grain surface, increasing the flame spreading velocity, for the same quasi steady state pressure. In fact, during the first phase of the SRM start-up, the higher mass flow rate from the igniter defines a higher pressure growth rate of the chamber, and also an increase of convective heating of the propellant surface of the entire impingement region. Therefore, the higher heat fluxes entail a shorter first ignition time and also a shorter ignition of the grain propellant surface (faster flame spreading inside the impingement region).

Moreover, the earlier pressure growth of the chamber implies an earlier nozzle seal rupture. This last occurs with a higher HEP level, which indicates the onset of more non uniform flow field conditions, in comparison with the reference cases. In the meanwhile, the different igniter MFR laws produce similar flame spreading velocities in the standard region, as result

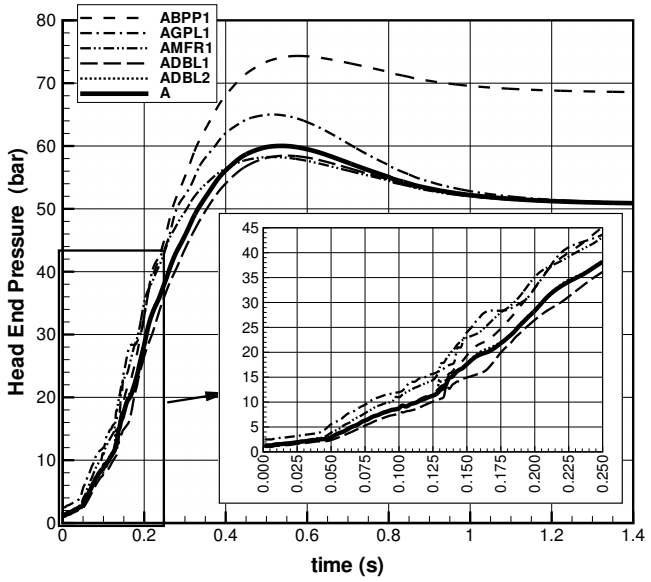

Figure 8: Head End Pressure during Start-up for SRM A - Parametric Analysis cont'd

of the combination of the propellant heating due to flame radiation from neighbor regions of ignited propellant and convective heat fluxes due to igniter jets far from the impingement region, which are not altered in a relevant way by the modification of the mass flow rate coming from the igniter. A different distribution in time of the igniter MFR causes also a different distribution in time of the erosive burning effects within the impingement region. Hence, for a higher maximum value of the mass flow rate (and lower time Δt of constant region for the igniter mass flow rate, in order to keep constant the igniter propellant mass - see Fig. 3), an increase of the pressure growth rate occurs in the first part of the ignition transient, caused by an increase of the erosive burning within the impingement region. On the other hand, a lower pressure overshoot occurs during the end of the IT, since the igniter mass flow rate in this time interval becomes lower than the one of the baseline configurations, reducing consequently also the erosive burning inside the impingement region. The opposite behavior occurs for the cases with a reduction of the maximum mass flow rate of the igniter - AMFR2 and BMFR2 cases.

For both the SRMs configurations, a different igniter nozzles configuration (50 % axial - 50 % radial mass flow rate distribution - cases AIC1 and BIC1, see Figs. 8 and Fig. 9) does not alter in a relevant manner the ignition transient of the SRM A and SRM B. Going in a deepened analysis, the small differences in the HEP curve are related to a slightly different ignition sequence/flame spreading velocity of the propellant grain, especially in the impingement region, which is caused by the different distribution of the igniter energy in the flowfield, in terms of the direction of the igniter jets. For the same reason, some small differences are also present in the erosive burning effects, which dictate the shape of the pressure overpeak in both the SRMs. In general terms, both these effects are very small.

A higher pressurization level of the chamber (cases AGPL1 for SRM A and BGPL1 for SRM B, see Figs. 8 and Fig. 9) causes a slight earlier first ignition time instant of the grain propellant surface. Indeed, it implies a little lower expansion of the igniter lateral jets and a more concentrated impingement region, which, in turn, brings about a slight increase of the convective heating, responsible for the faster first ignition of the propellant grain surface. In the meanwhile, the flame spreading process occurs with almost the same velocity in the impingement region and a slight faster and slower one, respectively in the head-end region and the standard region, leading to a small translation in time of the HEP curve, in comparison with the baseline configurations. In the same time, the AGPL1 case is affected by a higher erosive burning in the impingement region, because of the higher velocities of the igniter jets impinging the propellant surface. This explains also the higher pressurization rate of the chamber during the whole ignition transient and the higher pressure overshooting, in comparison with the reference cases, for both the SRM configurations.

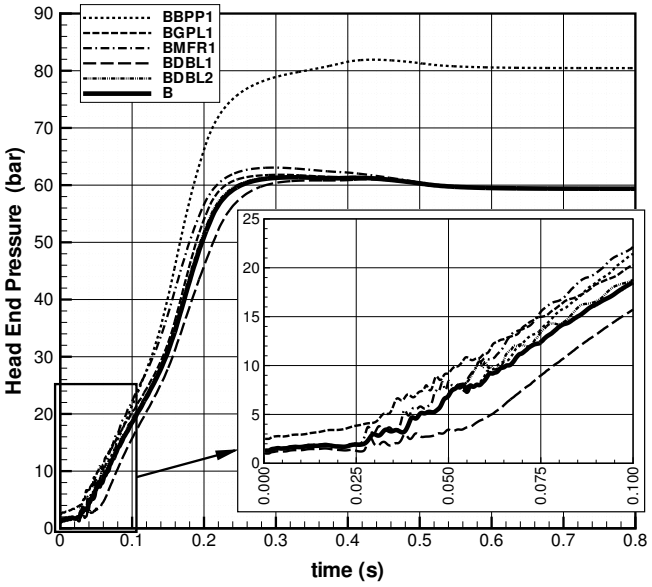

Figure 9: Head End Pressure during Start-up for SRM B - Parametric Analysis cont'd

The discussion of the effects of a different nozzle seal configuration has to be made separately for the two design options considered: a no-seal configuration (ADBL1 and BDBL1) and a nozzle seal able to resist up to 8 bar before being broken up (7 bar of differential pressure) - ADBL2 and BDBL1 (see Fig. 8 and Fig. 9). Apart the effects of such different designs on the pressure oscillations onset during the SRM start-up, which are discussed in the related part of the analysis, a different configuration of the nozzle seal has not relevant effects on the ignition transient of the SRMs, for both the baseline motor configurations. More precisely, the open chamber configuration, because of the absence of the seal and, with very second order of importance, the slight lower level of the pressure in the chamber at the initial conditions of the SRM (1 bar instead of 1.3 bar) brings to a slower ignition of the whole combustion surface, which causes, in turn, a slightly different lower pressure and pressurization rate of the combustion chamber. Whereas, a higher level

of differential pressure for the nozzle seal rupture, excluding the time instant around the occurrence of the seal breaking itself, has almost negligible effects on the overall ignition transient of the SRMs.

5.2.1. SRM Design Parameters affecting Pressure Oscillations Onset

In the following, the discussion will analyze separately the two SRMs, depicting the design parameters which play a role in the pressure oscillations onset, in terms of their complete suppression, or in reducing/increasing their amplitude. For this purpose, it is worth recalling that the baseline SRM A is not prone to relevant pressure oscillations, but to a slight excitation of the chamber first acoustic mode caused by the nozzle seal breakage; whereas for the baseline SRM B, the ignition transient is characterized, during its pre-IT, by relevant pressure oscillations, before the occurrence of the nozzle seal rupture.

Segmented SRM. For the reference SRM A, the segmented SRM, an enhancement of pressure oscillations with respect to the reference SRM A is outlined (see Fig. 10), before the nozzle seal breaking, for a complete redesign of the SRM geometry (AMSG1 case). This case is of particular interest since it underlines as, in order to have the onset of pressure oscillations during the ignition transient, the presence of traveling waves in the chamber is condition only necessary, but not sufficient. In fact, with respect to the baseline configuration A, different propagation phenomena occur inside the different bore geometry, because of the absence of the slots and the submergence region. In particular, a more rapid pressure increase of the SRM aft part occurs for the AMSG1 case. Different timings and interactions of the waves generated by the igniter occur in the chamber, leading to the sudden increase of the SRM HEP at ≈ 0.11 s (Fig. 10). This is due to the compression wave generated by the igniter jets, which travels downward the SRM axis (head-to-aft) and is reflected by the nozzle seal, before its breaking up. This pressure wave, moving backwards towards the SRM head-end, interacts with the igniter jets and reaches the head end at ≈ 0.11 s, suddenly increasing the HEP. Afterwards, it is reflected by the head end and interacts again with the igniter jets creating some other small fluctuations in the HEP (after ≈ 0.11 s, in Fig. 10).

For the reference SRM A, after the nozzle seal breaking, a modification of the small but present pressure oscillations triggered by the seal breakage event can be obtained (in a similar way to the reference SRM B, as will be discussed in the following) with the use of a different pressurizing gas (helium - APGT1 case) or with a higher pressurizing gas pressurization level (AGPL1 case).

The effect caused by the use of a different pressurizing gas (APGT1 case), even if small, is intrinsically related to the lower acoustic impedance of the helium in comparison with the nitrogen, which brings about the presence of a more uniform flowfield inside the chamber at the time of nozzle seal breakage. This, in turn, entails to have a slightly stronger expansion wave impinging on the head-end of the SRM, which travels forth and back, before being damped by the flame spreading and the whole chamber pressurization.

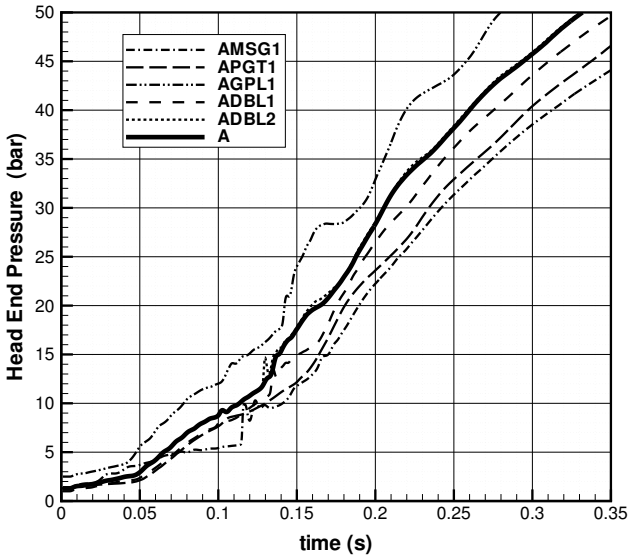

Figure 10: Design Parameters Affecting Pressure Oscillations during Ignition Transient: Segmented SRM A

In the same manner, the moderate increase of the HEP oscillations amplitude for the AGPL1 case (higher initial pressurization) is due to the following scenario. For the AGPL1 case, because of the higher initial pressure inside the chamber, a slightly faster ignition of the propellant grain surface occurs, implying a higher average pressure level inside the chamber and more non uniform conditions in the bore. Therefore, since traveling in a flow field with slightly higher spatial gradients, the expansion wave generated by the seal breakage induces oscillations with a slightly higher amplitude, which are then damped in a longer time interval during the flame spreading and chamber filling phases of the IT.

The ADBL1 and ADBL2 cases merit a brief comment related to the particular behavior of the HEP at ≈ 0.13 - 0.14 s (Fig. 10), that is represented by a relative maximum during the HEP increase. Indeed, a similar effect can not be seen in the HEP of the reference SRM A, which, in the same time window, is monotonically increasing. For both these cases, the root cause of this small peak is the compression wave generated by the igniter, which is partially reflected by the nozzle and moves upstream reaching the head-end of the SRM. In fact, this wave is more intense than the one arising for the reference SRM A and, interacting with the cavities and igniter jets structure at the head end of the SRM, it produces this particular shape of the HEP.

Finocyl SRM. The pressure oscillations occurring during the first part of the ignition transient are due to the system of waves generated at the transit of the igniter jets across the finocyl entrance section, as recalled in section 4.2. Instead, the pressure oscillations occurring after the nozzle seal breakage are brought about the expansion wave generated by the in-out differential pressure at the time when the seal is blown away, which reaches

the SRM head-end (for a deepened description and analysis of both such phenomena, refer to Refs. [5–15]).

The remedies to the pressure oscillations onset in SRMs with finocyl geometries, during the first part of the ignition transient were deeply analyzed and identified in the works [7–9, 17], and will be briefly recalled in the following of this paper.

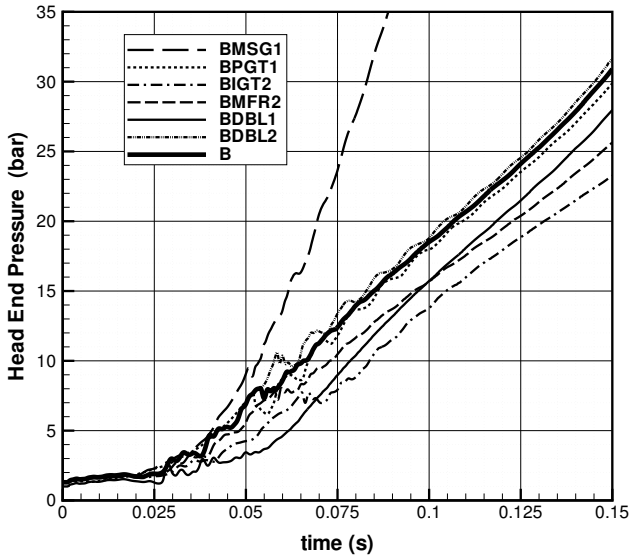

Figure 11: Design Parameters Affecting Pressure Oscillations during Ignition Transient: Finocyl SRM `B`

The motor geometry (`BMSG1` case) and, in particular, the use of a geometry of the propellant grain with a constant port area, instead of the aft-finocyl one, completely avoids the onset of the pressure oscillations, before the nozzle seal breaking and reduce the ones occurring after it. This effect is owed to the removal of the intrinsic mechanism of generation of the acoustic waves which cause the pressure oscillations in the SRM: the geometrical variation of the bore in the aft-part of the SRM, with which the igniter jets material surface interacts bringing about the generation of pressure waves in case of the aft-finocyl geometry.

In the same manner, the pressurizing gas type (`BPGT1` case), and in particular, the use of a different pressurizing gas, helium other than the classical nitrogen, completely destroys the mechanism of onset the pressure oscillations before the nozzle seal breaking, by removing the interaction of the igniter jets material surface, within a medium in which exists a relevant variation of the acoustic impedance at the entrance of the finocyl region. On the contrary, the use of helium as pressurizing gas enhances a little the amplitude of the pressure oscillations triggered by the nozzle seal rupture. Indeed, because of this more uniform flowfield due to the use of the helium as pressurizing gas, the expansion wave originated from the nozzle seal breakage reaches the head-end having a higher intensity and, consequently, excites the chamber first acoustic mode with a higher energy, which needs more time to be damped down, during the flame spreading and chamber filling phases.

Either a different distribution of the igniter mass flow rate law in time (`BMFR2` case) or a smaller igniter total enthalpy injected in the chamber (`BIGT2` case) do not avoid the pressure oscillations onset during the pre-IT of the SRM, but rather a slight reduction of their amplitude, since in both cases, a lower energy is delivered from the igniter into the flow, to be converted into acoustic energy. Both these design options of the SRM (igniter mass flow rate and energy) have not any significant effects on the pressure wave generated by the nozzle seal breakage, since they do not alter the seal rupture phenomenon, if not for second order and almost negligible effects.

On the contrary, an open chamber configuration (`BDBL1` case), while enhancing a little the pressure waves amplitude during the pre-IT, does not entail, as expected, any other pressure oscillations during the SRM start-up (because no nozzle seal breakage occurs). Instead, a higher seal breakage level (`BDBL2`) implies the generation of a more intense expansion, when the nozzle seal breaks up and, in turn, a slight more intense activation of the chamber first acoustic mode, rapidly damped during the flame spreading and the chamber filling phases.

6. Conclusions

The start-up is a crucial phase in the operational life of solid rocket motors, because of the complex and tightly coupled unsteady phenomena which, starting from the first activation of the igniter, bring the motor to be fully ignited and in its quasi-steady conditions. Indeed, the ignition transient of SRM can have important impacts in terms of the dynamic environment for all the structures of the launcher, and especially for the payload, as well as in terms of the mission itself, for multi-stage or multi-booster launcher configurations.

This works has presented a very detailed parametric analysis of the effects on the SRM start-up phase of the main design options of a motor: the propellant grain shape; the burning rate and the energy of the propellant grain; the igniter configuration and energy; the pressurizing gas type and the initial pressurization level; the nozzle seal configuration (or open chamber configuration). Two baseline configurations have been selected: a three-segment SRM, similar to the Ariane 5 solid booster and an aft-finocyl SRM, similar to VEGA Zefiro SRMs, for applications like solid stage or small booster. These two baseline configurations are chosen intentionally to discuss two different applications of the solid rocket motors in a launch vehicle. In particular, in order to discuss the design parameters which drive the onset of pressure oscillations during the ignition transient, the aft-finocyl SRM is on purpose designed prone to relevant pressure oscillations in the first phase of the motor start-up.

The analysis of the results indicates that except for known and trivial effects (e.g. the effect of a faster/slower propellant burning rate on the quasi steady pressure; or a more energetic igniter, on a more rapid first ignition of the propellant and so on), the effects of a design parameter modification on the behavior of the SRM during the IT has to be carefully extrapolated to other SRM configurations. Hence, general recommendations are difficult to be drawn out, especially for SRM configuration different from the ones analyzed in this work, because the SRM

IT is strongly dependent on the SRM configuration under analysis and the phenomena involved during the motor start-up are strongly non-linear and inter-related each other.

Considering the possible onset of pressure oscillations during the SRM start-up, two kinds of mechanisms are source of pressure fluctuations inside the SRM, that are the result of the excitation of the chamber fundamental frequencies (mainly the first acoustic mode): 1) during the pre-ignition transient of aft-finocyl SRMs, the interaction of the igniter jets with the finocyl entrance region, in presence of a non-uniform flowfield in the chamber; 2) typically, later in time, the nozzle seal rupture, in both the segmented SRM and the finocyl one. This analysis exploited all the efforts of knowledge and understanding of such phenomena for VEGA solid rocket motors, which turned out the proposal by the work-group at Sapienza University of Rome of the use of the helium as pressurizing gas, which has been successfully validated with the VEGA solid rocket motors static firing tests, from 2005 to 2010 and the qualification flights in 2012 and 2013.

Therefore, in aft-finocyl SRMs, the pressure oscillations onset can be avoided by the use of the helium, as pressurizing gas, or avoiding the presence of the geometrical variation related to the finocyl region. A slight control of the pressure oscillations amplitude can be obtained by reducing the energy of the igniter transferred to the flowfield.

On the contrary, for the segmented SRM, which is not prone to pressure oscillations during the pre-ignition transient, a modification of the SRM internal geometry of the propellant grain, or the nozzle seal breakage level can induce a relevant HEP gradient in time, because of the timing and interaction of the pressure wave generated by the igniter with the nozzle with the chamber, the seal breakage and the ignition of the propellant grain.

Considering, instead, the pressure oscillations generated by the nozzle seal breakage, for both the three-segments SRM and the aft-finocyl SRM, the use of helium as pressurizing gas and a higher level for the nozzle seal breakage level bring about an increase in the pressure oscillations amplitude and a more intense chamber first mode activation, due to the seal rupture. In the meanwhile, as very straightforward implication, no pressure oscillations appears with the removal of the nozzle seal with an open chamber configuration.

Acknowledgements

This work was supported by the ESA-ESTEC/Contract No. 22711/09/NL/RA "Simulation models for solid rocket motor (SRM) ignition transient (IT)"[23].

[1] M. Di Giacinto, F. Serraglia, Modeling of Solid Motor Start-up, AIAA Paper 2001-3448, DOI: 10.2514/6.2001-3448, 2001, 37^{th} AIAA Jt. Propul. Conf. and Exhib.

[2] M. Di Giacinto, F. Serraglia, Modeling of SRM Ignition Transient: Role of the Main Phenomena, AIDAA, 2001, *XVI* Natl. Con.

[3] M. Di Giacinto, Numerical Simulation of Solid Motor Ignition Transient, no. 5-ISICP-027-8-pp-MDG, Begell House Inc., New York, 2001, 2002, 5^{th} Int. Symp. on Spec. Top. in Chem. Prop.

[4] B. Favini, M. Di Giacinto, F. Serraglia, Solid Rocket Motor Ignition Transient Revisited, in: Proc. of the 8^{th} Int. Workshop on Combust. and Prop., 2002, Pozzuoli, Italy.

[5] B. Favini, F. Serraglia, M. Di Giacinto, Modeling of Flowfield Features During Ignition of Solid Rocket Motors, AIAA Paper 2002-3753, DOI: 10.2514/6.2002-3753, 2002, 38^{th} AIAA Jt. Propul. Conf. and Exhib.

[6] B. Favini, M. Di Giacinto, F. Serraglia, Acoustic Phenomena During SRM Ignition Transient, IN-SPACE PROPULSION I-19032, 2003, 10-IWCP 10^{th} Int. Workshop on Combust. and Propuls.

[7] B. Favini, F. Serraglia, M. Di Giacinto, A. Neri, Pressuring Gas Effects on Pressure Oscillations during the Ignition Transient of SRM, EUCASS, 2005, 1^{st} Eur. Conf. for Aerosp. Sci.

[8] F. Serraglia, B. Favini, M. Di Giacinto, A. Neri, Gas Dynamic Features in Solid Rocket Motors with Finocyl Grain during Ingnition, in: SP-563 Proc. of 5^{th} Eur. Symp. on Aerothermodyn. for Space Veh., ESA/DLR, 2004.

[9] B. Favini, M. Di Giacinto, F. Serraglia, Ignition Transient Pressure Oscillations in Solid Rocket Motors, AIAA Paper 2005-4165, DOI: 10.2514/6.2005-4165, 2005, 41^{st} AIAA Jt. Propul. Conf. and Exhib.

[10] B. Favini, M. Di Giacinto, A. Attili, D. Scoccimarro, M. Biagioni, R. De Amicis, A. Neri, P. Bellomi, S. Bianchi, F. Serraglia, M. Bonnet, Ignition Transient Induced Loads Control Strategy for VEGA Launcher' Solid Rocket Motors: the Zefiro 9 Static Firing Test Predictions and Post Firing Analysis, AIAA Paper 2006-5277, DOI: 10.2514/6.2006-5277, 2006, 42^{nd} AIAA Jt. Propul. Conf. and Exhib.

[11] M. Di Giacinto, B. Favini, A. Attili, F. Serraglia, D. Scoccimarro, C. Di Trapani, Internal Ballistics and Dynamics of VEGA Launcher Solid Rocket Motors During Ignition Transient: Firing Test Predictions and Post Firing Analysis, AIAA 2007-5814, DOI: 10.2514/6.2007-5814, 2007, 43^{rd} AIAA Jt. Propul. Conf. and Exhib.

[12] A. Attili, B. Favini, M. Di Giacinto, F. Serraglia, Analysis of Ignition Transient of VEGA Launcher Motors, Space Propulsion 2008, 2008, 5^{th} Int. Spacecr. Prop. Conf.- 2^{nd} Int. Symp. on Prop. for Space Transp.

[13] B. Favini, A. Attili, V. Ferretti, M. Di Giacinto, F. Serraglia, Post-Firing Analysis of Z23 SRM Ignition Transient, AIAA 2009-5511, DOI: 10.2514/6.2009-5511, 2009, 45^{th} AIAA Jt. Propul. Conf. and Exhib.

[14] B. Favini, F. Serraglia, E. Cavallini, V. Ferretti, M. Di Giacinto, Thrust Anomalies at Ignition Transient of Solid Propellant Rockets, no. IAC-10.C4.2.4, Int. Astronaut. Fed., 2010, 61^{st} Int. Astronaut. Con., ISBN: 9781617823688.

[15] M. Di Giacinto, B. Favini, E. Cavallini, F. Serraglia, Lessons Learnt during the Development of VEGA Launcher Solid Rocket Motors, Int. Astronaut. Fed., 2012, 63^{rd} Int. Astronaut. Con. - ISBN: 9781622769797.

[16] S. Gordon, B. McBride, Computer Program for Calculation of Complex Chemical Equilibrium Compositions and Applications, NASA Ref. Publ. 1311, Part 1: Analysis and Part 2: Users Manual and Program Description (October 1994).

[17] B. Favini, S. Zaghi, F. Serraglia, M. Di Giacinto, 3D Numerical Simulation of Ignition Transient in SRM, AIAA Paper 2006-4953, DOI: 10.2514/6.2006-4953, 2006, 42^{nd} AIAA Jt. Propul. Conf. and Exhib.

[18] B. Favini, S. Zaghi, M. Di Giacinto, F. Serraglia, A Fully Three Dimensional Analysis of Pre-Ignition Transient in Solid Rocket Motors, AIAA Paper 2007-5781, DOI: 10.2514/6.2007-5781, 2007, 43^{rd} AIAA Jt. Propul. Conf. and Exhib.

[19] S. Zaghi, B. Favini, M. Di Giacinto, F. Serraglia, 3D Simulations of Pre-Ignition Transient of P80 SRM, AIAA Paper 2008-4606, DOI: 10.2514/6.2008-4606, 2008, 44^{th} AIAA Jt. Propul. Conf. and Exhib.

[20] S. Zaghi, B. Favini, M. Di Giacinto, F. Serraglia, Ignition Transient of Vega Solid Rocket Motors, Space Propulsion 2008, 2008, 5^{th} Int. Spacecr. Prop. Conf.- 2^{nd} Int. Symp. on Prop. for Space Transp.

[21] S. Zaghi, B. Favini, A. Attili, M. Di Giacinto, F. Serraglia, Comparison Between Different Pressurant Gases for Ignition Transient of P80 SRM, AIAA Paper 2009-4980, DOI: 10.2514/6.2009-4980, 2009, 45^{th} AIAA Jt. Propul. Conf. and Exhib.

[22] S. Zaghi, B. Favini, E. Cavallini, M. Di Giacinto, F. Serraglia, On the Effects of Supersonic Igniter Jets during Pre-Ignition Transient of SRMs, AIAA 2010-6583, DOI: 10.2514/6.2010-6583, 2010, 46^{th} AIAA Jt. Propul. Conf. and Exhib.

[23] E. Cavallini, B. Favini, M. Di Giacinto, Improvements towards SRM Ignition Transients, Final Report and Executive Summary Report of ESTEC/Contract N. 22711/09/NL/RA "Simulation Models for Solid Rocket Motor (SRM) Ignition Transient (IT)", Dept. of Mech. and Aeros. Eng. - Sapienza Univ. of Rome (2012).